Cellular Physiology and Biochemistry

Cell Physiol Biochem 2015;35:259-269
DOI: 10.1159/000369693
Published online: January 09, 2015
Accepted: November 19, 2014

1421-9778/15/0351-0259$39.50/0

Original Paper

Pamidronate Attenuates Diastolic Dysfunction Induced by Myocardial Infarction Associated with Changes in Geometric Patterning

Andréa F. Gonçalves[a] Luiz Henrique Congio[a] Priscila P. dos Santos[a] Bruna P. M. Rafacho[a] Bruna L. B. Pereira[a] Renan F. T. Claro[a] Nara A. Costa[a] Fernanda Chiuso-Minicucci[b] Paula S. Azevedo[a] Bertha F. Polegato[a] Katashi Okoshi[a] Elenize J. Pereira[a] Marina P. Okoshi[a] Sergio A. R. Paiva[a] Leonardo A. M. Zornoff[a] Marcos F. Minicucci[a]

[a]Internal Medicine Department, Botucatu Medical School, Univ Estadual Paulista (UNESP), Botucatu, [b]Department of Microbiology and Immunology, Institute of Biosciences, Univ Estadual Paulista (UNESP), Botucatu, Brazil

Key Words
Ventricular remodeling • Bisphosphonates • Calcium handling proteins

Abstract
Background/Aims: The aim of this study was to evaluate the influence of pamidronate on ventricular remodeling after myocardial infarction. ***Methods:*** Male Wistar rats were assigned to four groups: a sham group, in which animals were submitted to simulated surgery and received weekly subcutaneous injection of saline (S group; n=14); a group in which animals received weekly subcutaneous injection of pamidronate (3 mg/kg of body weight) and were submitted to simulated surgery (SP group, n=14); a myocardial infarction group, in which animals were submitted to coronary artery ligation and received weekly subcutaneous injection of saline (MI group, n=13); and a myocardial infarction group with pamidronate treatment (MIP group, n=14). The rats were observed for three months. ***Results:*** Animals submitted to MI had left chamber enlargement and worse diastolic and systolic function compared with SHAM groups. E/A ratio, LV posterior and relative wall thickness were lower in the MIP compared with the MI group. There was no interaction between pamidronate administration and MI on systolic function, myocyte hypertrophy, collagen content, and calcium handling proteins. ***Conclusion:*** Pamidronate attenuates diastolic dysfunction following MI.

Marcos F Minicucci

Botucatu Medical School, Rubião Júnior s/n, Botucatu, SP, CEP: 18618-970 (Brazil)
Tel. +55 14 38222969, Fax +55 14 38222238, E-Mail minicucci@fmb.unesp.br

Introduction

Acute coronary syndrome remains the leading cause of death worldwide. In 2009, approximately 683,000 patients were discharged from US hospitals with this diagnosis. In addition, one-year mortality of ST-elevation myocardial infarction (MI) is approximately 7 to 18% [1, 2]. Epidemiological studies have reported that 40% of MI are accompanied by left systolic ventricular dysfunction and 25% by signs and symptoms of heart failure [3, 4]. Several factors influence the development of ventricular dysfunction and overt heart failure, among them, ventricular remodeling is the most important [4].

Ventricular remodeling is defined by genomic expression and molecular, cellular and interstitial changes that are manifested clinically as changes in size, shape and function of the heart after cardiac injury [5, 6]. Initially, remodeling may contribute to the maintenance of cardiac function, however, chronic ventricular remodeling leads to progressive ventricular dysfunction and sudden death [6]. Several factors are associated with ventricular remodeling after MI; inflammation, cell death and extracellular matrix content all play an important role in this scenario[6]. Thus, interventions that modulate these pathways could attenuate the ventricular remodeling process and improve prognosis.

Bisphosphonates (BPs) are stable analogues of inorganic pyrophosphate, an endogenous regulator of calcium metabolism. These compounds have been used widely in the treatment of disorders associated with excessive bone resorption, such as hypercalcemia of malignancy and multiple myeloma [7, 8]. BP structures contain two phosphonate groups attached to a single carbon atom, forming a "P-C-P" structure. In addition, bisphosphonates have two lateral chains (R1 and R2) attached to the central carbon atom [7, 8]. First generation BPs or non-nitrogen containing BPs, by the action of class II aminoacyl–transfer RNA synthetases, are converted into a toxic ATP analogue; leading to osteoclast and macrophage apoptosis. Pamidronate is a second generation bisphosphonate with an amino group in R2 lateral chain. These BPs inhibit the activity of farnesyl pyrophosphate synthase (FPPS), a key enzyme in the mevalonate pathway and directly catalyzes the synthesis of FPP and geranylgeranyl pyrophosphate (GGPP), which are required for the post-translational modifications of some intracellular proteins that control the translation of signaling, proliferation and cell death [9].

Recently, experimental and clinical studies have shown additional biological effects from these compounds. BPs can modulate inflammatory processes and reduce matrix metalloproteinase activity and adhesion molecule expression [9]. Experimental studies suggest that BPs reduce macrophage production of nitric oxide, tumor necrosis factor alpha and interleukine-1 [10]. Makkonem et al. demonstrated that this anti-inflammatory effect of BPs occurs partially due to NFκ-B inhibition [11]. In addition, the administration of BPs to experimental models of atherosclerosis reduced vascular calcification and interfered with the function of arterial smooth muscle, attenuating vascular remodeling [12, 13]. However, observational clinical studies have produced contradictory results regarding BPs therapy and MI risk [14-16].

Few studies have evaluated the influence of BPs on the ventricular remodeling process. Hwang et al. showed that the administration of zoledronate to female Sprague-Dawley rats one day before coronary ligation had no effect in the early period after the coronary occlusion [17]. Yang et al. also showed that BPs attenuate cardiac hypertrophy and fibrosis induced by angiotensin II [18]. Importantly, no study has evaluated the effect of BPs treatment in the chronic remodeling process after MI. Thus the aim of this study was to evaluate the influence of pamidronate on ventricular remodeling after coronary occlusion.

Materials and Methods

All of the experiments and procedures were performed in accordance with the National Institute of Health's Guide for the Care and Use of Laboratory Animals and were approved by the Animal Ethics Committee of Botucatu Medical School.

Male Wistar rats weighing 200-250 g were assigned to four experimental groups: a sham group, in which animals were submitted to simulated surgery and received weekly subcutaneous injections of saline (S group; n=14); a group in which animals received weekly subcutaneous injections of pamidronate (3 mg/kg of body weight) [19] and were submitted to simulated surgery (SP group, n=14); a myocardial infarction group, in which animals were submitted to coronary artery ligation and received weekly subcutaneous injections of saline (MI group, n=13); and a myocardial infarction group with pamidronate treatment (MIP group, n=14). An echocardiographic exam was performed seven days after myocardial infarction, and there was no morphological or functional difference between the MI groups (data not shown). The treatment was administrated to the rats after the first echocardiogram. Water was supplied *ad libitum*. The rats were observed for three months, after which morphological, functional and biochemical analyses were performed.

Coronary artery ligation

When the animals achieved body weights of 200-250 g, myocardial infarction was induced as previously described [20, 21]. Briefly, the rats were anesthetized with ketamine (70 mg/kg) and xylazine (1 mg/kg), and after a left thoracotomy, the heart was exteriorized. The left atrium was retracted to facilitate the ligation of the left coronary artery with 5-0 mononylon between the pulmonary outflow tract and the left atrium. The heart was then replaced in the thorax, and the lungs were inflated by positive pressure as the thoracotomy was closed. The rats were housed in a temperature-controlled room (24°C) with a 12-h light:dark cycle.

Echocardiographic analysis

After three months, all of the animals were weighed and evaluated by a transthoracic echocardiographic exam. All of the measurements were made by the same observer, according to the leading-edge method recommended by the American Society of Echocardiography/ European Association of Echocardiography [22]. The end-systolic and end-diastolic cavity areas were calculated as the sum of the areas from both the short- and long-axis views in diastole (SumD) and systole (SumS), respectively. The fractional area change (FAC) was calculated from the composite cavity areas as follows: FAC = (SumD-SumS)/SumD. The relative wall thickness (RWT) was determined as 2*posterior wall thickness/end-diastolic diameter. The velocities of transmitral diastolic flow (E and A velocities) were obtained from the apical four-chamber view. The E/A ratio, the isovolumetric relaxation time and the isovolumetric relaxation time corrected by the heart rate ($IRT/RR^{0,5}$) were used as indices of LV diastolic function.

Morphometric analysis

Upon completion of the functional analyses, the right and left ventricles (including the interventricular septum) were dissected, separated and weighed. Transverse sections of the LV were fixed in 10% buffered formalin and paraffin-embedded. Five-micron-thick sections were stained with hematoxylin and eosin (HE). The myocyte cross-sectional area (CSA) was determined for a minimum of 100 myocytes per H&E-stained cross section. The measurements were obtained from digital images (400 × magnification) that were collected with a video camera attached to a Leica microscope; the images were analyzed with the Image-Pro Plus 3.0 software program (Media Cybernetics; Silver Spring, MD). The myocyte cross-sectional area was measured with a digital pad, and the selected cells were transversely cut so that the nucleus was in the center of the myocyte [23, 24]. The interstitial collagen fraction (ICF) was determined for the entire cardiac section that was stained with Picrosirius Red. The lengths of the infarcted and viable muscle for both the endocardial and epicardial circumferences were determined by planimetry. Infarct size was calculated by dividing the endocardial and epicardial circumferences of the infarcted area by the total epicardial and endocardial ventricular circumferences. The measurements were performed on midventricular sections (5-6 mm from the apex) under the assumption that the left midventricular slice shows a close linear relation with the sum of the area measurements from all of the heart sections [25].

Zymography

The metalloproteinase (MMP)-2 and -9 activity was determined as previously reported [26]. In brief, samples for analysis were prepared by dilution in extraction sample buffer consisting of 50 mM Tris, pH 7.4; 0.2 M NaCl; 0.1% Triton X and 10 mM $CaCl_2$. Then, they were diluted in application sample buffer consisting of 0.5 M Tris, pH 6.8; 100% glycerol; and 0.05% bromophenol blue. The samples were loaded into the

wells of 8% SDS-polyacrylamide containing 1% gelatin. Electrophoresis carried out in a Bio-Rad apparatus at 80 V for 2 h, when bromophenol blue reaches the bottom of the gel. The gel was removed and washed two times with 2.5% Triton-X-100 and then washed with 50 mM Tris pH 8.4. The gel was then incubated at 37°C overnight in activation solution consisting of 50 mM Tris pH 8.4; 5 mM $CaCl_2$ and Zn Cl_2. The staining was performed for 2 h with 0.5% coomassie blue and destained in 30% methanol and 10% acetic acid until clear bands over a dark background were observed. Staining and destaining were performed at room temperature on a rotatory shaker. The gels were photographed and the intensity of gelatinolytic action (clear bands) analyzed in a UVP, UV, White Darkhon image analyzer.

Western blot analysis

Left ventricular samples were extracted using Tris-Triton buffer (10 mM Tris (pH 7.4), 100 mM NaCl, 1 mM EDTA, 1 mM EGTA, 1% Triton X-100, 10% glycerol, 0.1% SDS, 0.5% deoxycholate, 1 nM EDTA, 1 mM EGTA and a mixture of protease inhibitors, 1 mM sodium orthovanadate, 1 mM sodium fluoride and 1% leupeptin, aprotinin, pepstatin) to detect Serca2a, Phospholamban (PLB) total and phospho-Ser16-PLB, Na^+/Ca^{2+} exchanger, L-type Ca^{2+} channel, and periostin. The samples were then centrifuged at 12000 at 4 °C for 20 min, and the supernatant was collected. The supernatant protein content was quantified using the Bradford method. The samples were separated on a 10% SDS-polyacrylamide gel, and the proteins were transferred to a nitrocellulose membrane. The membrane was blocked with 5% nonfat dry milk in Tris-buffered saline containing Tris 1 M (pH 8.0), NaCl 5 M and Tween 20 at room temperature for 2 h. The membrane was then incubated with the following antibodies: primary antibody anti-Serca2a, rabbit polyclonal IgG (Abcam, Inc., Canada, ab 3625), anti-phospholamban total, mouse monoclonal (Thermo Scientific, Inc., US, 3922), anti-phospho-Ser16- PLB, rabbit polyclonal (Abcam, Inc., Canada, ab 15000), anti-Na^+/Ca^{2+} exchanger, mouse monoclonal (Thermo Scientific, Inc., US, MA 151051), anti- L-type Ca^{2+} channel CP21C (H-280), rabbit polyclonal IgG (Santa Cruz Biotechnology, Inc., Europe, sc 25686), and anti-periostin (goat polyclonal IgG (Santa Cruz Biotechnology, Inc., Europe, sc 49480)). The membrane was washed with TBS and Tween 20 and incubated with the appropriate secondary peroxidase-conjugated antibody. A Super Signal® West Pico Chemiluminescent Substrate (Pierce Protein Research Products, Rockford, USA) was used to detect bound antibodies. GAPDH (GAPDH (6C5), mouse monoclonal IgG1, (Santa Cruz Biotechnology, Inc., Europe, sc 32233) was used for normalization.

Myocardial tissue metalloproteinase inhibitor-1 concentration

The levels of TIMP-1 in the heart homogenates were evaluated by ELISA according to the manufacturer's instructions (R & D Systems, Minneapolis, MN, USA).

Statistical analysis

The data are expressed as the means ± SD. Comparisons between groups were performed by two-way ANOVA analysis followed by Holm-Sidak. For infarct size comparison, Student's t-test was performed. The data analysis was carried out with SigmaStat for Windows v2.03 (SPSS Inc., Chicago, IL). The significance level was set at $P < 0.05$.

Results

There was no difference in infarct size between the MI and MIP groups (MI: 29.9 ± 9.4 % *vs.* MIP: 28.8 ± 10.4 %; p=0.806). Thus, this variable did not influence our results. Only two animals of the MI group and two of the MIP group died during the follow-up.

Echocardiographic analysis

Morphological and functional echocardiographic data are presented in Table 1. The animals submitted to MI had higher values of left atrium and ventricle, corrected by body weight, compared with the SHAM groups. Diastolic and systolic functions were also worse in the MI groups. Groups treated with pamidronate had higher A waves in comparison with groups that received saline. LV posterior wall thickness (PWT) and relative wall thickness (RWT) were lower in the MIP group compared with the MI group (Fig. 1). In addition, peak

Table 1. Echocardiographic data. P: pamidronate; MI: myocardial infarction; BW: body weight; HR: heart rate; TL: tibial length; LVDD: LV end-diastolic dimension; LVSD: LV end-systolic dimension; PWT: LV posterior wall thickness; RWT: relative wall thickness; IVRT/$RR^{0.5}$: isovolumetric relaxation time corrected for heart rate; E/A: peak velocity of early ventricular filling/ peak velocity of transmitral flow during atrial contraction; EDT: E wave deceleration time; FAC: fractional area change; FS: fractional shortening; PWSV: posterior wall shortening velocity. *data normalized for statistical analysis. $ IMP group ≠ IM group, & SP group ≠ IMP group, § IM group ≠ S group

	S group (n= 14)	SP group (n= 14)	MI group (n= 11)	MIP group (n= 12)	p MI	p P	p MIxP
BW (g)	427.9 ± 43.0	421.1 ± 20.2	470.5 ± 26.4	454.6 ± 33.7	< 0.001	0.216	0.616
HR (bpm)	253.4 ± 35.4	294.3 ± 47.3	276.5 ± 27.9	280.1 ± 33.3	0.670	0.040	0.083
TL (cm)	3.9 ± 0.1	4.2 ± 0.1&	4.2 ± 0.2§	4.1 ± 0.1$	0.006	<0.001	0.005
LA/BW (mm/kg)	13.8 ± 1.8	13.4 ± 1.7	15.6 ± 3.1	17.1 ± 2.4	< 0.001	0.412	0.157
LVDD (mm)	8.5 ± 0.6	8.6 ± 0.5	10.6 ± 1.0	10.9 ± 0.9	<0.001	0.390	0.794
LVDD/TL (mm/cm)	2.0 ± 0.2	2.2 ± 0.1	2.5 ± 0.3	2.7 ± 0.2	<0.001	0.009	0.541
LVDD/BW (mm/kg)	20.0 ± 1.9	20.5 ± 1.8	22.7 ± 2.4	24.0 ± 2.2	< 0.001	0.108	0.493
LVSD (mm)	4.3 ± 0.6	4.1 ± 0.6	8.3 ± 1.3	8.7 ± 1.1	<0.001	0.618	0.199
LVSD/TL(mm/cm)	1.0 ± 0.2	1.1 ± 0.2	2.0 ± 0.3	2.1 ± 0.3	< 0.001	0.148	0.308
LVSD/BW (mm/cm)	10.0 ± 1.2	9.7 ± 1.5	17.6 ± 2.9	19.3 ± 2.7	< 0.001	0.277	0.106
PWT (mm)	1.47 ± 0.07	1.52 ± 0.07&	1.94 ± 0.23§	1.79 ± 0.17$	< 0.001	0.262	0.019
RWT	0.35 ± 0.03	0.35 ± 0.03	0.37 ± 0.05	0.33 ± 0.03$	0.762	0.081	0.030
IRT/$RR^{0.5}$ (ms)	60.23 ± 8.09	64.03 ±7.78	59.90 ± 11.48	64.56 ± 10.91	0.972	0.121	0.871
E wave (cm/s)*	87.36 ± 8.52	95.07 ± 9.97	104.18 ± 25.97	92.42 ± 25.04	0.367	0.724	0.059
A wave (cm/s)*	53.86 ± 15.32	64.86 ± 15.45	43.27 ± 25.39	63.67 ± 24.40	0.071	0.005	0.208
E/A*	1.74 ± 0.52	1.52 ± 0.27	3.92 ± 3.21§	1.61 ± 1.05$	0.017	0.008	0.027
EDT (ms)	44.92 ± 6.64	41.70 ± 7.03	38.55 ± 7.35	42.27 ± 4.78	0.145	0.898	0.082
FAC	71.43 ± 5.29	75.15 ± 4.47	40.43 ± 12.19	36.67 ± 8.50	< 0.001	0.992	0.098
FS (%)	49.7 ± 3.9	52.7 ± 6.0	22.6 ± 6.2	20.1 ± 4.4	< 0.001	0.876	0.064
PWSV (mm/s)	39.87 ± 5.61	42.15 ± 3.51	27.77 ± 7.30	26.53 ± 5.21	< 0.001	0.736	0.258

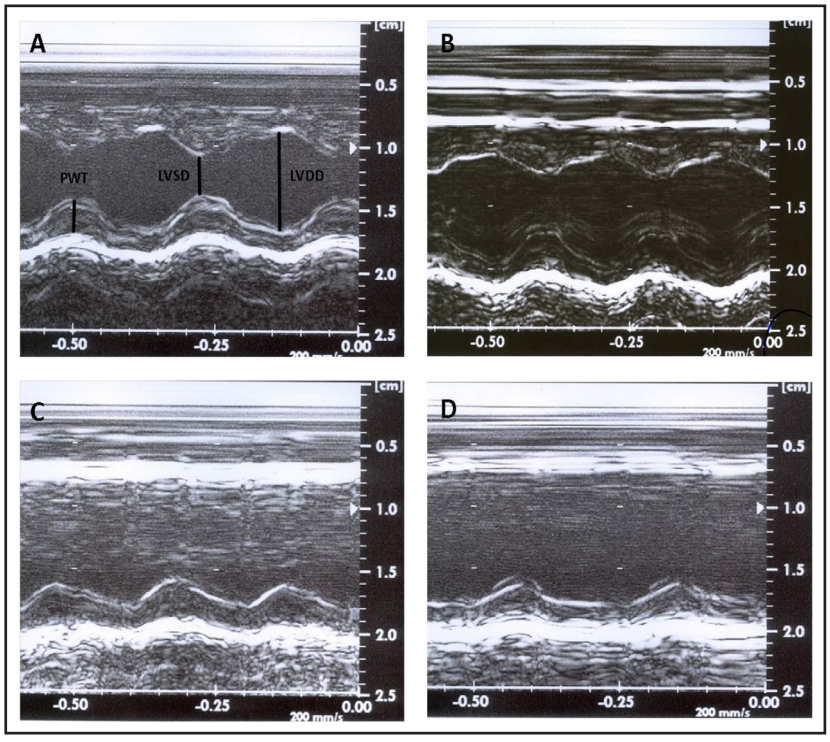

Fig. 1. Echocardiographic analysis. M-mode images of left ventricle (LV). PWT: LV posterior wall thickness; LVDD: LV end-diastolic dimension; LVSD: LV end-systolic dimension. A: sham group; B: SP group (weekly subcutaneous injections of pamidronate + simulated surgery); C:MI group (coronary artery ligation + weekly subcutaneous injections of saline); D: MIP group (myocardial infarction + pamidronate treatment). LVDD, LVSD and PWT were higher in animals submitted to MI. MIP group had lower PWT compared with MI group (p<0.05).

velocity of early ventricular filling/ peak velocity of transmitral flow during atrial contraction (E/A) was also lower in the MIP group compared with the MI group. There was no interaction between pamidronate administration and MI in variables that evaluate systolic function.

Table 2. Morphological data and myocardial MMPs and TIMP-1. P: pamidronate; MI: myocardial infarction; BW: body weight; LVW: left ventricular weight; RVW: right ventricular weight; ICF: interstitial collagen fraction; CSA: myocyte cross-sectional area; TIMP-1: tissue metalloproteinase inhibitor-1; MMP: matrix metalloproteinase. *data normalized for statistical analysis. # (S group=8; SP group=9; MI group=9; MIP group=10)

	S group (n= 7)	SP group (n= 7)	MI group (n= 7)	MIP group (n= 7)	p MI	p P	p MIxP
LVW/BW (g/mg)#	1.96 ± 0.13	2.08 ± 0.21	2.24 ± 0.38	2.23 ± 0.28	0.018	0.554	0.503
RVW/BW (g/mg)*#	0.63 ± 0.10	0.60 ± 0.13	0.85 ± 0.33	0.76 ± 0.28	0.018	0.414	0.787
ICF (%)*	4.4 ± 1.5	2.2 ± 1.8	5.6 ± 4.0	5.9 ± 3.1	0.024	0.242	0.115
CSA (μm^2)	295.0 ± 59.7	298.9 ± 41.2	338.3 ± 40.3	354.0 ± 51.8	0.021	0.626	0.768
TIMP-1 (pg/g of protein)*	68.2 ± 48.5	55.8 ± 15.8	103.7 ± 98.4	97.7 ± 60.1	0.160	0.999	0.739
MMP-2 active/total*	75.5 ± 10.7	79.0 ± 9.2	76.5 ± 9.8	74.1 ± 13.1	0.850	0.858	0.282
MMP-9 active/total*	14.3 ± 8.7	8.6 ± 7.1	7.7 ± 4.3	7.8± 5.5	0.256	0.295	0.324

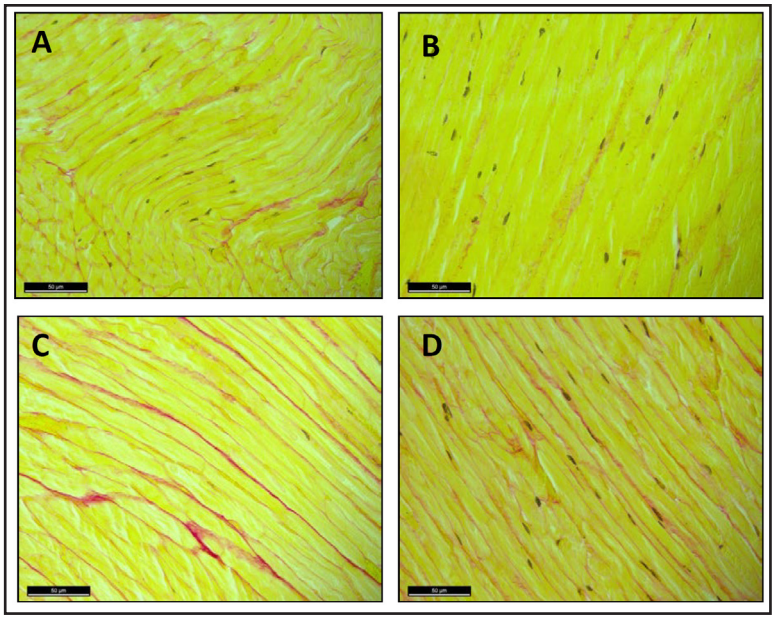

Fig. 2. Interstitial collagen fraction in picrosirius red stained cardiac section – red colour for collagen fibres, yellow for myocytes. A: sham group; B: SP group (weekly subcutaneous injections of pamidronate + simulated surgery); C:MI group (coronary artery ligation + weekly subcutaneous injections of saline); D: MIP group (myocardial infarction + pamidronate treatment). Lens magnification 400X. Animals submitted to MI had higher amount of collagen content ($p<0.05$). However, pamidronate supplementation did not influence this variable.

Morphometric analysis

The morphological data are listed in Table 2. MI groups had higher left (LVW) and right ventricular weight (RVW) compared with SHAM groups. In addition, interstitial collagen fraction (Fig. 2) and myocyte cross-sectional area (Fig. 3) were also higher in the animals submitted to MI.

Zymography and TIMP-1 concentration

There were no differences between the groups in matrix metalloproteinase activity and tissue metalloproteinase inhibitor-1 (TIMP-1) concentration in myocardium. No effect of pamidronate was observed in these variables (Table 2).

Western blot analysis

Myocardial periostin was lower in the non MI group compared with the MI groups. On the other hand, pamidronate did not affect this variable (Fig. 4).

Regarding calcium handling proteins, the MI groups had lower myocardial concentrations of Serca2a and higher concentrations of phospho-PLB/total and of Na^+/Ca^{2+} exchanger, compared with SHAM groups. There was no interaction between pamidronate and MI in these variables (Fig. 5).

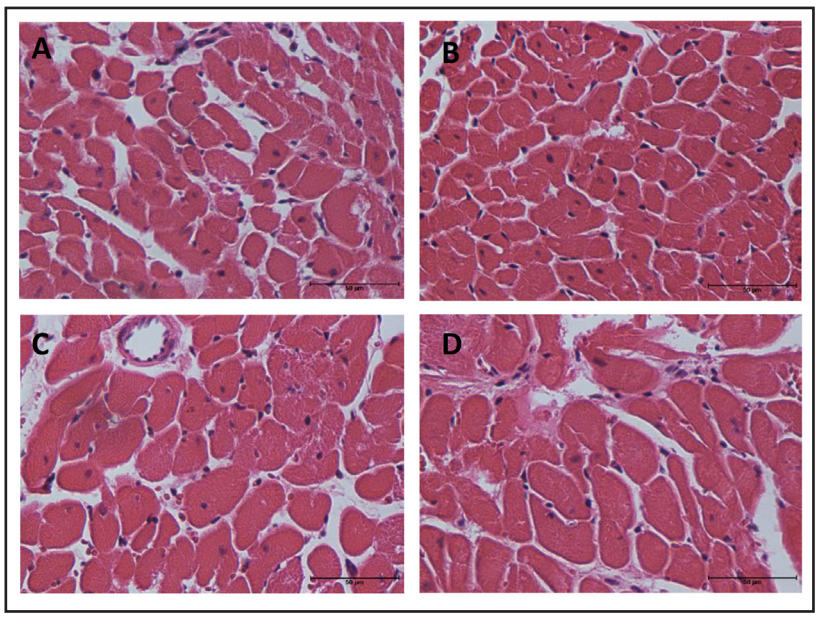

Fig. 3. Myocyte cross-sectional area (CSA), H&E-stained. A: sham group; B: SP group (weekly subcutaneous injections of pamidronate + simulated surgery); C:MI group (coronary artery ligation + weekly subcutaneous injections of saline); D: MIP group (myocardial infarction + pamidronate treatment). Animals submitted to MI had higher values of CSA ($p<0.05$). Lens magnification 400X. However, pamidronate supplementation did not influence this variable.

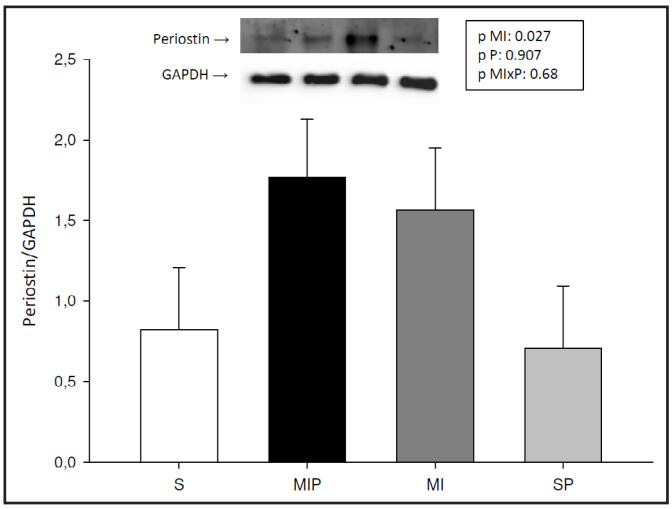

Fig. 4. Western blot analysis for left ventricle periostin concentration. S: sham group; SP group (weekly subcutaneous injections of pamidronate + simulated surgery); MI group (coronary artery ligation + weekly subcutaneous injections of saline); MIP group (myocardial infarction + pamidronate treatment). There is no interaction between pamidronate and MI. However, periostin was lower in the non MI group compared with the MI groups. In addition, pamidronate did not affect this variable.

Discussion

The objective of this study was to evaluate the influence of pamidronate on ventricular remodeling after myocardial infarction. Our data showed that pamidronate attenuated diastolic dysfunction following MI due to changes in geometric patterns. In addition, cardiac extracellular matrix content and calcium handling proteins did not participate in this process.

As expected, MI groups presented with left cardiac chamber enlargement and with worse diastolic and systolic functions compared with SHAM groups. The treatment with pamidronate (3 mg/kg of body weight) once a week reduced LV posterior and relative wall thickness. Alterations in ventricular mass, volume and geometry after cardiac injury can be interpreted as representative variables of the remodeling process [5, 6]. Thus, pamidronate attenuated ventricular remodeling following MI. To our knowledge there is only one study that evaluates the effect of BPs following MI, and the administration of zoledronate one day before coronary ligation did not influence ventricular remodeling [17].

An important issue is that attenuation of the remodeling process should be associated with improved cardiac function. Indeed, diastolic dysfunction was also improved by BP treatment in our study. Several variables could interfere with diastolic function, such as

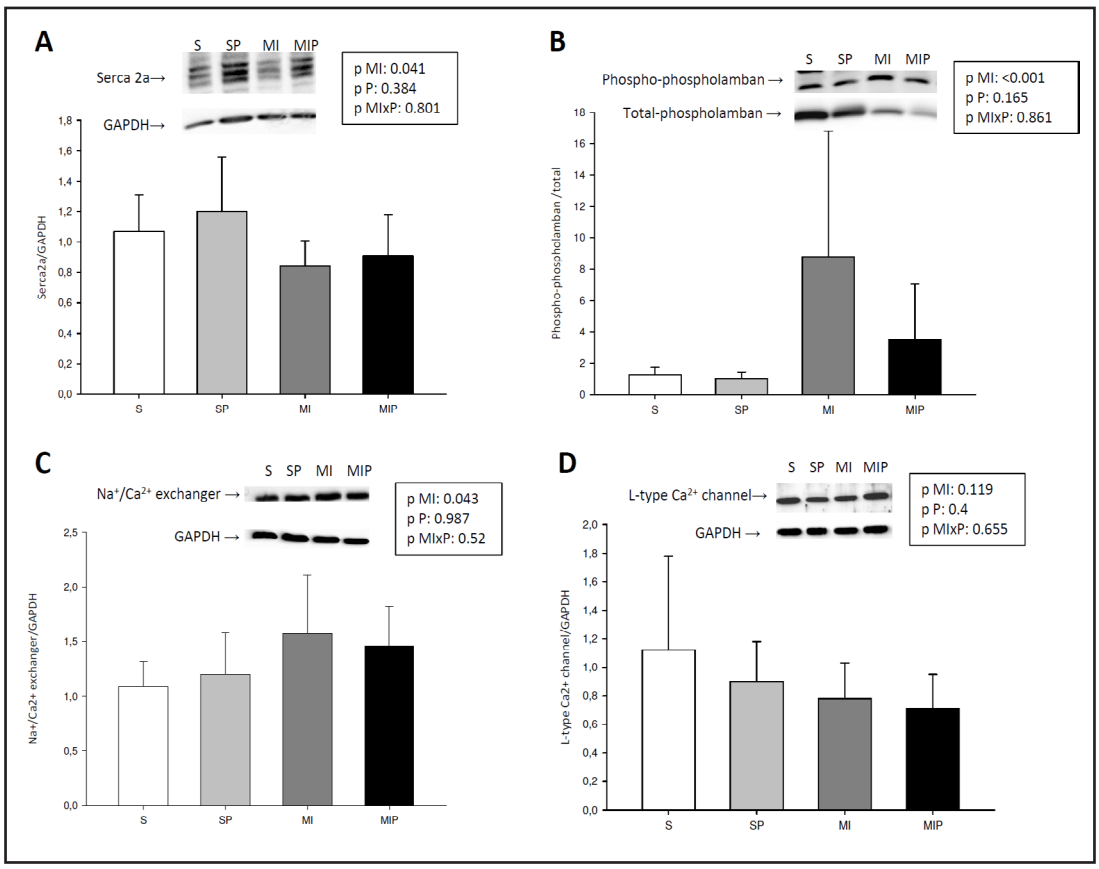

Fig. 5. Western blot analysis for calcium handling proteins. S:sham group; SP group (weekly subcutaneous injections of pamidronate + simulated surgery); MI group (coronary artery ligation + weekly subcutaneous injections of saline); MIP group (myocardial infarction + pamidronate treatment). There was no interaction between pamidronate and MI in these proteins. The MI groups had lower myocardial concentrations of Serca2a and higher concentrations of phospho-PLB/total and of Na^+/Ca^{2+} exchanger, compared with SHAM groups.

changes in geometric pattern, interstitial collagen content, calcium handling proteins and ATP availability [27].

Considering the potential mechanisms involved in the improved diastolic function induced by BP, the treatment was associated with a reduction in LV relative wall thickness. One potential mechanism to explain this effect is that pamidronate inhibits the activity of farnesyl pyrophosphate synthase, a key regulatory enzyme in cell proliferation [9]. Therefore, our data suggest that modifications in LV geometric pattern could explain the attenuation of diastolic dysfunction in this model of MI.

Another variable that can influence diastolic function is the interstitial collagen content. Collagen is one of the most important components of extracellular matrix (ECM). The ECM is a fibrillar network that embeds myofibers and the whole cardiac structure. It is composed by different proteins such as collagen, fibronectin, proteoglycan, components of basement membrane, proteases and growth factors [28]. An important component of ECM is a family of extracellular matrix enzymes, metalloproteinases (MMPs). MMPs are a family of over 25 species of zinc-dependent proteases that play an important role in collagen degradation. The activity of MMPs is controlled by the action of specific MMPs inhibitors or TIMPs, particularly TIMP-1 [29]. Some studies that investigated the anti-neoangiogenic activity of BPs showed that these drugs inhibit endothelial growth factors and MMP-2 and MMP-14 [30, 31]. In addition, other studies have demonstrated *in vitro* and *in vivo* evidence that BPs attenuate

cardiac hypertrophy and fibrosis induced by angiotensin II [18, 32]. However, in our study, pamidronate administration did not influence myocardial TIMP-1 concentration or MMP-2 and MMP-9 activity. In addition, there was no effect of this BP on interstitial collagen content and on myocyte hypertrophy following MI.

Intracellular calcium participates both in the control of the contractile process and in the coupling between mechanical activity, energy metabolism and protein synthesis [27]. In this scenario, calcium handling protein controls its own homeostasis. Some proteins such as L-type Ca^{2+} and ryanodine channels are responsible for the increase in cytoplasmic free calcium concentration and for adequate LV contraction [33, 34]. Additionally, to allow ventricular relaxation, there is a reuptake of Ca^{2+} into the sarcoplasmic reticulum by SERCA2 and removal of Ca^{2+} from the cell by the Na+/ Ca^{2+} exchanger. The activity of SERCA2 is regulated by phospholamban. In its unphosphorylated state, phospholamban inhibits SERCA2 activity. However, after phospholamban phosphorylation, this inhibition is diminished and increases Ca^{2+} reuptake [33-35]. In experimental models of atherosclerosis, BPs reduced vascular calcification and interfered with the function of arterial smooth muscle, most likely via L-type Ca^{2+} channel [12, 13, 36]. In our study, SERCA2 concentration was lower after MI. The decrease of this protein was correlated with the increase of Na+/ Ca^{2+} exchanger and Phospho-PLB. There was no difference in L-type Ca^{2+} channel in MI groups when compared with SHAM groups. The treatment with pamidronate did not influence these variables.

Some limitations of this study should be noted. Firstly, we did not evaluate the animals during the whole process. We assessed echocardiographic and morphometric variables, periostin, MMPs, TIMP1 and calcium handling proteins only three months following MI. In addition, we did not assess FPP and GGPP levels in the heart tissue. Therefore the mechanism of pamidronate effects on cardiac remodeling after coronary occlusion remains to be elucidated.

In conclusion, pamidronate attenuates diastolic dysfunction following MI.

Acknowledgments

This study was funded by the “Fundação de Amparo à Pesquisa do Estado de São Paulo” FAPESP (2011/10328-8)

Disclosure Statement

There is no conflict of interest.

References

1 O'Gara PT, Kushner FG, Ascheim DD, Casey DE, Jr., Chung MK, de Lemos JA, Ettinger SM, Fang JC, Fesmire FM, Franklin BA, Granger CB, Krumholz HM, Linderbaum JA, Morrow DA, Newby LK, Ornato JP, Ou N, Radford MJ, Tamis-Holland JE, Tommaso JE, Tracy CM, Woo YJ, Zhao DX: 2013 accf/aha guideline for the management of st-elevation myocardial infarction: Executive summary: A report of the american college of cardiology foundation/american heart association task force on practice guidelines. Circulation 2013;127:529-555.

2 Jernberg T, Johanson P, Held C, Svennblad B, Lindback J, Wallentin L: Association between adoption of evidence-based treatment and survival for patients with st-elevation myocardial infarction. JAMA 2011;305:1677-1684.

3 Albert NM, Lewis C: Recognizing and managing asymptomatic left ventricular dysfunction after myocardial infarction. Crit Care Nurse 2008;28:20-37; quiz 38.

4 Minicucci MF, Azevedo PS, Polegato BF, Paiva SA, Zornoff LA: Heart failure after myocardial infarction: Clinical implications and treatment. Clin Cardiol 2011;34:410-414.
5 Cohn JN, Ferrari R, Sharpe N: Cardiac remodeling--concepts and clinical implications: A consensus paper from an international forum on cardiac remodeling. Behalf of an international forum on cardiac remodeling. J Am Coll Cardiol 2000;35:569-582.
6 Zornoff LA, Paiva SA, Duarte DR, Spadaro J: Ventricular remodeling after myocardial infarction: Concepts and clinical implications. Arq Bras Cardiol 2009;92:157-164.
7 Russell RG, Rogers MJ: Bisphosphonates: From the laboratory to the clinic and back again. Bone 1999;25:97-106.
8 Drake MT, Clarke BL, Khosla S: Bisphosphonates: Mechanism of action and role in clinical practice. Mayo Clin Proc 2008;83:1032-1045.
9 Corrado A, Santoro N, Cantatore FP: Extra-skeletal effects of bisphosphonates. Joint Bone Spine 2007;74:32-38.
10 van Rooijen N, Sanders A, van den Berg TK: Apoptosis of macrophages induced by liposome-mediated intracellular delivery of clodronate and propamidine. J Immunol Methods 1996;193:93-99.
11 Makkonen N, Salminen A, Rogers MJ, Frith JC, Urtti A, Azhayeva E, Monkkonen J: Contrasting effects of alendronate and clodronate on raw 264 macrophages: The role of a bisphosphonate metabolite. Eur J Pharm Sci 1999;8:109-118.
12 Lomashvili KA, Monier-Faugere MC, Wang X, Malluche HH, O'Neill WC: Effect of bisphosphonates on vascular calcification and bone metabolism in experimental renal failure. Kidney Int 2009;75:617-625.
13 Wu L, Zhu L, Shi WH, Zhang J, Ma D, Yu B: Zoledronate inhibits the proliferation, adhesion and migration of vascular smooth muscle cells. Eur J Pharmacol 2009;602:124-131.
14 Pittman CB, Davis LA, Zeringue AL, Caplan L, Wehmeier KR, Scherrer JF, Xian H, Cunningham FE, McDonald JR, Arnold A, Eisen SA: Myocardial infarction risk among patients with fractures receiving bisphosphonates. Mayo Clin Proc 2014;89:43-51.
15 Kang JH, Keller JJ, Lin HC: Bisphosphonates reduced the risk of acute myocardial infarction: A 2-year follow-up study. Osteoporos Int 2013;24:271-277.
16 Wolfe F, Bolster MB, O'Connor CM, Michaud K, Lyles KW, Colon-Emeric CS: Bisphosphonate use is associated with reduced risk of myocardial infarction in patients with rheumatoid arthritis. J Bone Miner Res 2013;28:984-991.
17 Hwang H, Hale SL, Leeka J, Kloner RA: Effects of zoledronate in the repair of chronically infarcted rat myocardium. J Cardiovasc Pharmacol 2010;56:604-609.
18 Yang J, Zhu HH, Chen GP, Ye Y, Zhao CZ, Mou Y, Hu SJ: Inhibition of farnesyl pyrophosphate synthase attenuates angiotensin ii-induced cardiac hypertrophy and fibrosis in vivo. Int J Biochem Cell Biol 2013;45:657-666.
19 Jokihaara J, Porsti IH, Koobi P, Jolma PM, Mustonen JT, Saha HH, Sievanen H, Kannus P, Iwaniec UT, Turner RT, Jarvinen TL: Treatment of experimental renal osteodystrophy with pamidronate. Kidney Int 2008;74:319-327.
20 Minicucci MF, Azevedo PS, Martinez PF, Lima AR, Bonomo C, Guizoni DM, Polegato BF, Okoshi MP, Okoshi K, Matsubara BB, Paiva SA, Zornoff LA: Critical infarct size to induce ventricular remodeling, cardiac dysfunction and heart failure in rats. Int J Cardiol 2011;151:242-243.
21 Pfeffer JM, Finn PV, Zornoff LA, Pfeffer MA: Endothelin-a receptor antagonism during acute myocardial infarction in rats. Cardiovasc Drugs Ther 2000;14:579-587.
22 Lang RM, Bierig M, Devereux RB, Flachskampf FA, Foster E, Pellikka PA, Picard MH, Roman MJ, Seward J, Shanewise JS, Solomon SD, Spencer KT, Sutton MS, Stewart WJ: Recommendations for chamber quantification: A report from the american society of echocardiography's guidelines and standards committee and the chamber quantification writing group, developed in conjunction with the european association of echocardiography, a branch of the european society of cardiology. J Am Soc Echocardiogr 2005;18:1440-1463.
23 Azevedo PS, Minicucci MF, Chiuso-Minicucci F, Justulin LA, Jr., Matsubara LS, Matsubara BB, Novelli E, Seiva F, Ebaid G, Campana AO, Zornoff LA, Paiva SA: Ventricular remodeling induced by tissue vitamin a deficiency in rats. Cell Physiol Biochem 2010;26:395-402.

24 de Paiva SA, Zornoff LA, Okoshi MP, Okoshi K, Matsubara LS, Matsubara BB, Cicogna AC, Campana AO: Ventricular remodeling induced by retinoic acid supplementation in adult rats. Am J Physiol Heart Circ Physiol 2003;284:H2242-2246.
25 Minicucci MF, Azevedo PS, Oliveira SA, Jr., Martinez PF, Chiuso-Minicucci F, Polegato BF, Justulin LA, Jr., Matsubara LS, Matsubara BB, Paiva SA, Zornoff LA: Tissue vitamin a insufficiency results in adverse ventricular remodeling after experimental myocardial infarction. Cell Physiol Biochem 2010;26:523-530.
26 dos Santos PP, Nogueira BF, Rafacho BP, Azevedo PS, Polegato BF, Chiuso-Minicucci F, Bonomo C, Roscani MG, Zorzella-Pezavento SF, Tanni SE, Pereira EJ, Okoshi MP, Paiva SA, Zornoff LA, Minicucci MF: Aldosterone is not involved in the ventricular remodeling process induced by tobacco smoke exposure. Cell Physiol Biochem 2012;30:1191-1201.
27 Swynghedauw B: Molecular mechanisms of myocardial remodeling. Physiol Rev 1999;79:215-262.
28 Janicki JS, Brower GL: The role of myocardial fibrillar collagen in ventricular remodeling and function. J Card Fail 2002;8:S319-325.
29 Spinale FG: Matrix metalloproteinases: Regulation and dysregulation in the failing heart. Circ Res 2002;90:520-530.
30 Hamma-Kourbali Y, Di Benedetto M, Ledoux D, Oudar O, Leroux Y, Lecouvey M, Kraemer M: A novel non-containing-nitrogen bisphosphonate inhibits both in vitro and in vivo angiogenesis. Biochem Biophys Res Commun 2003;310:816-823.
31 Green JR, Clezardin P: Mechanisms of bisphosphonate effects on osteoclasts, tumor cell growth, and metastasis. Am J Clin Oncol 2002;25:S3-9.
32 Ye Y, Hu SJ, Li L: Inhibition of farnesylpyrophosphate synthase prevents angiotensin ii-induced hypertrophic responses in rat neonatal cardiomyocytes: Involvement of the rhoa/rho kinase pathway. FEBS Lett 2009;583:2997-3003.
33 Mudd JO, Kass DA: Tackling heart failure in the twenty-first century. Nature 2008;451:919-928.
34 Bers DM: Altered cardiac myocyte ca regulation in heart failure. Physiology (Bethesda) 2006;21:380-387.
35 Denipote F, Ardisson LP, Azevedo PS, Minicucci MF, Lima-Leopoldo AP, Chiuso-Minicucci F, Polegato BF, Matsubara BB, Matsubara LS, Novelli E, Paiva SA, Zornoff LA: Influence of taurine on cardiac remodeling induced by tobacco smoke exposure. Cell Physiol Biochem 2011;27:291-298.
36 Bevilacqua M, Dominguez LJ, Rosini S, Barbagallo M: Bisphosphonates and atherosclerosis: Why? Lupus 2005;14:773-779.